

Coherent X-Ray Diffractive Imaging: Modeling and Reconstruction

Oleg Gorobtsov, Moscow Institute of Physics and Technology, Russia

Supervisor: Dr. Adrian Mancuso, Leading Scientist, European XFEL GmbH

September 8, 2011

Contents

1	Introduction	3
2	Methods	4
2.1	Two-dimensional Plane Wave Imaging	4
2.1.1	Modelling	4
2.1.2	Reconstruction	5
2.2	Tomography	8
2.2.1	Modelling	8
2.2.2	Reconstruction	8
2.3	Three-dimensional CXDI	10
2.4	Two-dimensional Fresnel Imaging: Modelling	11
3	Conclusions and future work	13

1 Introduction

High resolution X-ray imaging, presently allowing resolution of up to 10 nm [2] for non-crystalline samples, aiming for much higher resolutions [5], is used in many fields of science, for example, to study both non-biological and biological samples - cells, viruses [1], etc. Three-dimensional (3D) imaging of thick samples, possible because of the high penetrative ability of the X-rays, provides insight in the objects structure much more so than a 2D projection.

Resolution of conventional x-ray imaging methods is often limited by the optics used, as it is difficult to produce x-ray lenses that are both efficient and highly resolving. [1] However, in coherent x-ray diffraction imaging the image is reconstructed directly from the far-field diffraction pattern, measured from an isolated object, without using optics between the sample and the detector. Resolution in this case is limited only by the wavelength and scattering angles recorded, and the technological problems concerning lens manufacture are removed.

On the other hand, coherent x-ray diffraction imaging, as its name suggests, introduces the need for coherence in the incident beam. Though experiments have been performed at the synchrotrons (for a review see [1]), free electron lasers are intrinsically much more spatially coherent [7].

Another reason why an FEL is very well-suited for coherent diffraction imaging is that the pulse duration of the photon bunches produced by FELs is in the order of hundreds of femtoseconds or, under certain conditions, even less than 10 femtoseconds. [4] This is important because samples suffer from radiation damage, which limits the resolution achieved at synchrotron sources, [5] however, extremely short and bright pulses can scatter from an object before the latter is destroyed. [3] [11] This means a further increase in the resolution of the reconstructed image, which relates to the exit surface wave of the sample, which contains the information about sample's structure.

The combination of ultrashort pulses and high spatial resolution at FELs can potentially be used to image macromolecules at near-atomic scales, which makes possible the structure determination of non-crystallized samples - for example, non-crystallized protein states. [2] [6]

The reconstruction of the image from the measured diffraction data, be it 2D or 3D, is not a trivial process. The detector measures only the intensity of the diffraction pattern, but to reconstruct an image, one also needs to reconstruct the phase of the wave at the plane of the detector. The aim of this work was to model the diffraction data and reconstruct the sample image for three different methods: 2D plane wave imaging, 3D CXDI and tomography from reconstructed 2D projections. In this project we simulate a very simple model of a cell component to test 3D CXDI and tomography for such a sample. This modelling program aims to ultimately evaluate the fidelity of reconstruction with a limited number of projections and a limited photon flux in each projection to explore the limitations radiation damage places on 3D Coherent Imaging with synchrotron sources.

2 Methods

2.1 Two-dimensional Plane Wave Imaging

2.1.1 Modelling

The general scheme is shown on Fig. 1. A plane wave is incident on a sample, which partly absorbs it and changes its relative phase at each point of the plane - according to the distribution of material in the sample. The wave propagates to the detector plane, where we see a far-field diffraction pattern. The distance z_{12} between sample and detector planes satisfy the condition $z_{12} \gg \frac{d^2}{\lambda}$, where d is the size of the sample and λ is the wavelength.

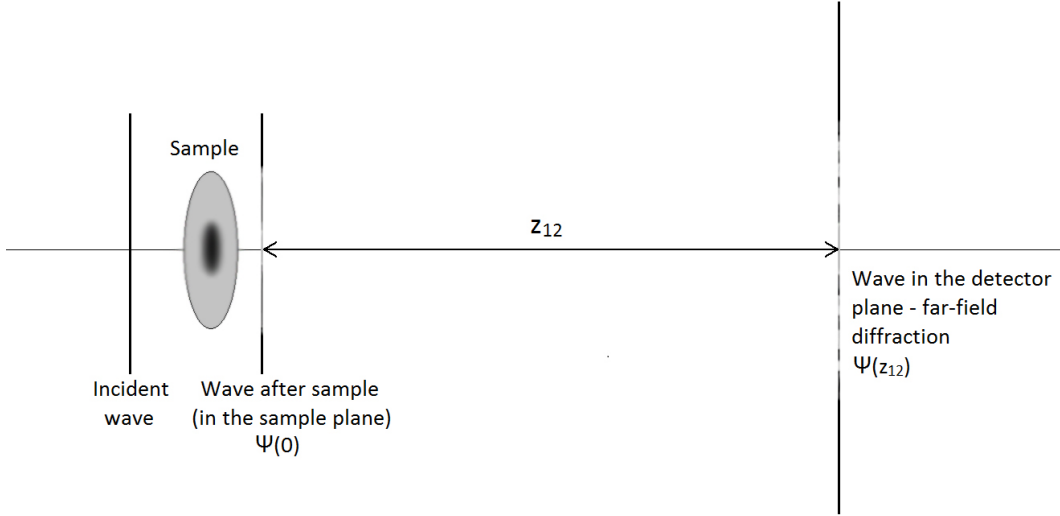


Figure 1: General scheme of plane-wave case propagation

The formula for propagation between planes is (for example, [9]):

$$\Psi(x'', y'', z_{12}) = \frac{i}{\lambda z_{12}} e^{\frac{2\pi i}{\lambda} z_{12}} e^{i\pi \lambda z_{12} (x''^2 + y''^2)} F\{\Psi(x', y', 0) e^{\frac{-i\pi}{\lambda z_{12}} (x'^2 + y'^2)}\},$$

where Ψ is a wave function, x' and y' are coordinates on the plane of origin, λ is the wavelength, z_{12} is the coordinate of the final plane relative to the original one, $x'' = \frac{x}{\lambda z_{12}}$ and $y'' = \frac{y}{\lambda z_{12}}$ are conjugate to x' and y' , F is the Fourier transform.

However, for calculations we need a discrete propagation formula. It follows from the previous one:

$$\Psi(l, k, z_{12}) = Prop(\Psi(m, n, 0), z_{12}) = \Psi i e^{\frac{2\pi i}{\lambda} z_{12}} e^{\frac{i\pi}{\lambda z_{12}} \rho_2^2} FFT\{\Psi(m, n, 0) e^{\frac{i\pi}{\lambda z_{12}} \rho_1^2}\},$$

where $\rho_1 = (m^2 + n^2)dx^2$ is distance from the center in the original plane, $\rho_2 = (l^2 + k^2)dx_2^2$ is distance from the center in the final plane, $dx_2 = \frac{\lambda z_{12}}{dxN}$ is pixel size in the final

plane, N - number of pixels, FFT - Fast Fourier Transform. It is important to point out that center of the Fourier transform in this formula is $\rho = 0$.

To model the far-field intensity, we need to perform following steps:

- 1. Construct the sample transmission function from the known properties and distribution of the materials in the sample
- 2. Multiply the incident wave function by it (assuming the sample is thin)
- 3. Propagate it to the detector plane according to the aforementioned formula
- 4. Calculate the diffracted intensity by squaring the far-field wave function

The sample transmission function is a product of the fraction not lost to the absorption and the factor corresponding to phase excursion.

The model sample used here is a simple model of a cell nucleus. It is described as a 1 micrometer sphere made of protein ($H_{50}C_{30}N_9O_{10}S_1$, density 1.35 g/cm^3) with a sphere of selenium with radius 200 nm inside, displaced from the center. The discrete sample transmission function is then:

$$Samp(l, k) = e^{\mu_N \sqrt{R_N^2 - \rho_{1N}^2} - (\mu_{Se} - \mu_N) \sqrt{R_{Se}^2 - \rho_{1Se}^2}} * e^{\frac{2i\pi}{\lambda} (2n_N \sqrt{R_N^2 - \rho_{1N}^2} + 2(n_{Se} - n_N) \sqrt{R_{Se}^2 - \rho_{1Se}^2})},$$

if $\rho_{1Se}^2 < R_{Se}^2$, otherwise

$$Samp(l, k) = e^{\mu_N \sqrt{R_N^2 - \rho_{1N}^2}} * e^{\frac{2i\pi}{\lambda} (2n_{Air} (R_N - \sqrt{R_N^2 - \rho_{1N}^2}) + 2n_N \sqrt{R_N^2 - \rho_{1N}^2})},$$

where R_{Se} is radius of the selenium sphere, R_N is radius of the protein sphere, x_{Se} and y_{Se} are coordinates of the selenium sphere, $\rho_{1Se} = ((l - x_{Se})^2 + (k - y_{Se})^2)^{1/2}$ is distance from the projection of the center of selenium sphere on the sample plane, $\rho_{1N} = (l^2 + k^2)^{1/2}$ is distance from the projection of the center of protein sphere on the sample plane, μ_N, μ_{Se} are absorption coefficients of protein and selenium on the given wavelength accordingly, and n_N, n_{Se} are differences of the refractive index from 1 for the same materials.

2.1.2 Reconstruction

To reconstruct the wave produced by the sample, we need to know not only the amplitude of the wave in the detector plane, but also the phase. This can be achieved by one of the iteration algorithms, using the original far-field intensity and the approximate size of the sample, known as its support. Those iterative algorithms converge[8], though sometimes to local minima, which do not correspond to the solution.

The simplest algorithm is called error-reduction. An intermediate wavefunction of the sample of iteration $n+1$ has the form:

$$\Psi_{n+1} = P_S P_F \Psi_n,$$

Here:

$$P_S \Psi(x) = \begin{cases} f(x), & x \in \text{Support} \\ 0, & \text{otherwise} \end{cases}$$

where Support is the approximate support of the beam in the sample plane. This essentially means that we don't want the reconstructed sample image to be outside the known sample borders.

$$P_F \Psi = \text{Prop}(\pi_F \text{Prop}(\Psi, z_{12}), -z_{12}),$$

where

$$\pi_F \Psi(x) = \begin{cases} A_{\text{measured}} e^{i\varphi_\Psi(x)}, & x \in \text{CSupport} \\ \Psi(x), & \text{otherwise} \end{cases}$$

Here A_{measured} is the square root of the far-field intensity, φ_Ψ is the phase of the wave function, CSupport is the area of the detector where measurements were made. This essentially means that on each iteration we keep the reconstructed detector wave function realistic.

However, this algorithm has a tendency to fall into local minima, and the so-called hybrid input-output algorithm is often used in the initial reconstruction:

$$\Psi_{n+1} = (P_S(\beta + 1) - \beta I) P_F \Psi_n,$$

where β is a scalar and I is the identity transformation.

The starting iteration is acquired by back-propagating the starting wavefunction in the detector plane (with randomly assigned phases in each pixel).

It is important to notice that the coefficients in the propagation formula can be dropped when iterating since, in this case, they cancel each other. This makes calculations significantly faster.

Shown on the Fig. 2 are the results of the reconstruction for the earlier modelled case. Here the number of iterations for HIO was 30, for ER 170, the support was a dish matching the incident wave in the sample plane, and CSupport was considered the whole detector plane. The wave incident on the sample was a dish of the constant phase and intensity.

Fig. 2 shows images for the wavelength of 7\AA , $z_{12} = 0.7m$, $dx = 24nm$, $N = 2048$, $\mu_N = 7.7 * 10^6 m^{-1}$, $\mu_{Se} = 2 * 10^8 m^{-1}$, $n_N = -9.8 * 10^{-5}$, $n_{Se} = -2.25 * 10^{-4}$.

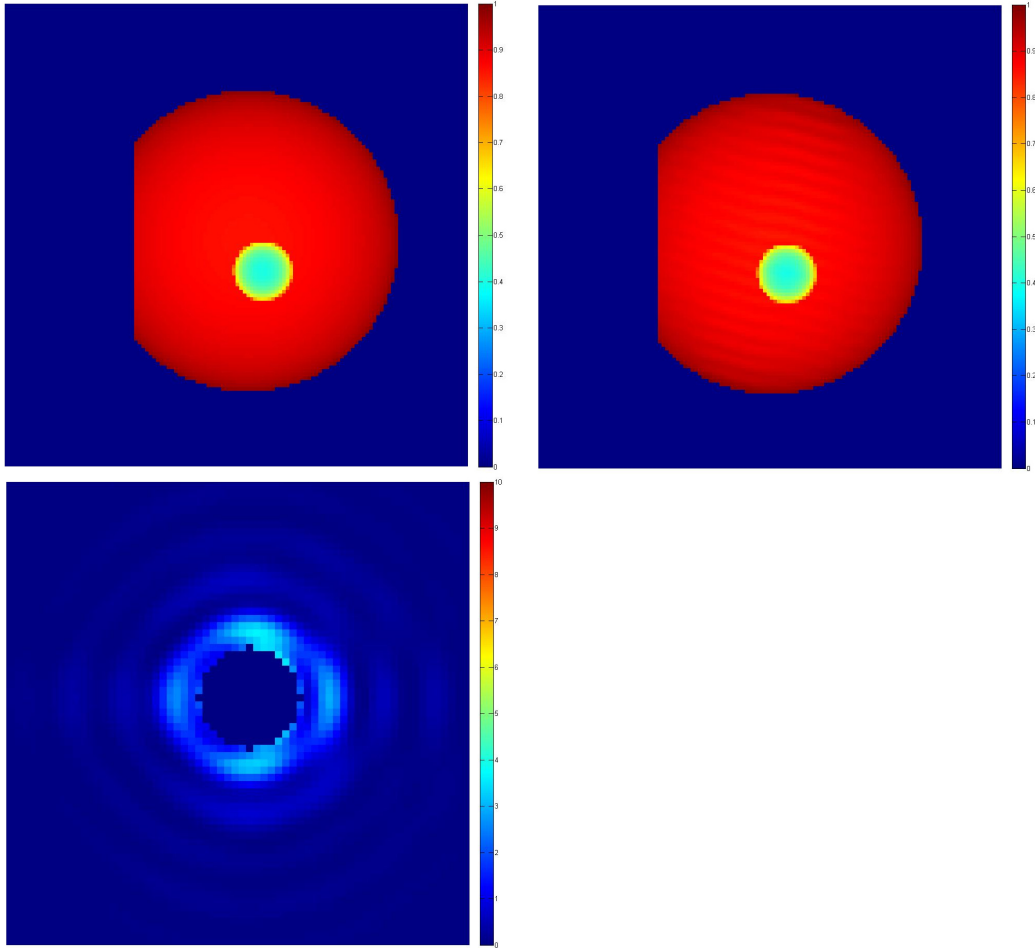


Figure 2: Original intensity in the sample plane; reconstructed intensity (scale is not the same); far-field intensity with central stop and Poissonian noise

2.2 Tomography

2.2.1 Modelling

The key difference in modelling the CXDI tomography and the 2D plane wave case is that for tomography we need to generate far-field intensities for different rotation angles of the sample. For a successful reconstruction, the number of rotations should be roughly equivalent to the number of resolution elements required in the depth dimension. [?] One difficulty arising here is that all of the stored images on the detector require a lot of memory, so for more efficient testing of the reconstruction program, each of the generated diffraction patterns was processed immediately after generation. The sample used was the same as in the 2D plane-wave case, with rotation angles from 0 to π , equally spaced and a total number of rotations of $N = 100$ - depth (in pixels) of the reconstructed volume.

2.2.2 Reconstruction

The reconstruction of each of the 2D proections of the sample is the same as in 2D case. However, to reconstruct the 3D volume of the object from those projections, we need to use a tomographical method. In this program, the filtered backprojection method[10] was used.

In the general case, formulaes for this method are

$$g'(s, \theta) = [F_S^{-1} abs * Rf](s, \theta),$$

$$f(x, y) = [Bg'](x, y),$$

where $f(x, y)$ is the 2D function which we want to reconstruct (slice of the sample), $Rf(s, \theta)$ is its projection on the axis rotated by the angle θ (this is what we really know), F is a Fourier transform, $abs(S, \theta) = |S|$, $Bg(x, y) = \int_0^\pi g(x \cos \theta + y \sin \theta, \theta) d\theta$.

Now one needs a discrete approximation for this set of formulae. The one used here is:

$$g'_n(m\Delta s) = \sum_i h(m - i)g_n(i),$$

$$[Bg'](x, y) = \frac{\pi}{N} \sum_n g'_n(x \cos n\frac{\pi}{N} + y \sin n\frac{\pi}{N}),$$

where

$$h(m) = \begin{cases} \frac{1}{4\Delta s}, & m=0 \\ 0, & m \text{ even and non-zero} \\ \frac{-1}{\pi^2 m^2 \Delta s^2}, & \text{otherwise} \end{cases}$$

, where N is the total number of rotations, Δs is the pixel size. It's important to notice that center here is in the point $n=0, m=0$. This was the algorithm for getting the slice of the sample in the horizontal plane from corresponding lines in the projection. To get the whole 3D image of the sample, one needs to perform this operation for all horizontal slices.

In Fig. 3 one can see how the filtered backprojection reconstructs direct projections. This is not the result of the filtered backprojection of the backpropagated intensities, however - as one could see from Fig. 2, for such a symmetrical sample some of them can be mirror images, and some - not, which obviously may lead to the corruption of the reconstruction.

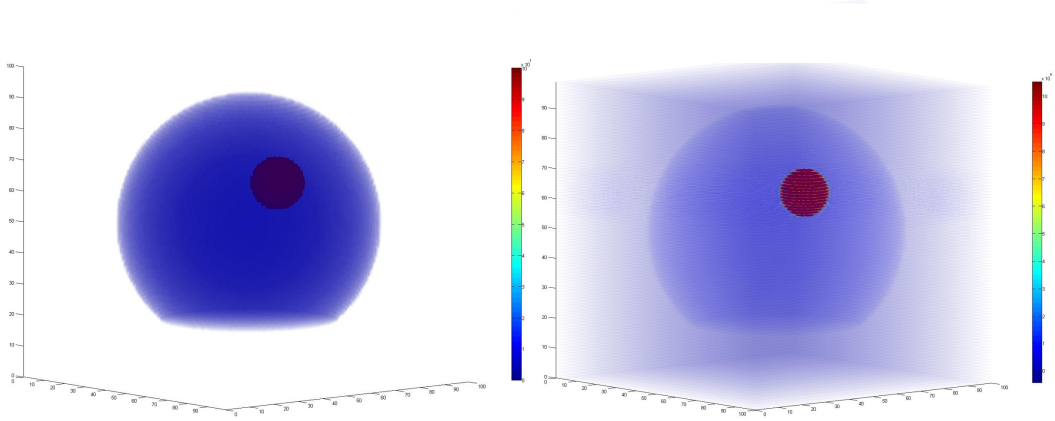


Figure 3: On the left is the original distribution of the real part of the refractive index; on the right is the filtered backprojection of the direct projections of the sample

2.3 Three-dimensional CXDI

In the case of three-dimensional coherent X-ray diffraction imaging we construct 3D intensity distribution in Fourier space. Due to the Fourier slice theorem, [10] the image on the detector, corresponding to the angle of rotation θ is rotated by the same angle in 3D Fourier space around the center. Using interpolation (in our case, nearest neighbor interpolation), we can calculate the intensity distribution in Fourier space. To make the result more accurate, one needs to get at least 1 plane going through any given pixel (oversampling)[2]:

$$\Delta\phi < \frac{\Delta x}{D},$$

where $\Delta\phi$ is angular increment, Δx is sampling interval in real space, and D is a maximum width of the sample along any of the real-space axis.

The modelling part is the same as in tomography case, since we also need to get far-field intensities from the rotated projections of the sample - the only difference is that number of projections required is higher. The reconstruction now begins from the preparational stage - creating a 3D array in Fourier space from the 2D projections with the aforementioned procedure. The iterative process now takes place in 3D space, and so the Fourier transform and all of the arrays are now generalized to the three-dimensional case. The algorithm formulae, however, remain the same as in 2D case.

The results of the reconstruction of the direct propagation you can see in Fig. 4. You can notice the mirror reflection and intensity variations, analogous to the once in the 2D-case and arising for the same reasons.

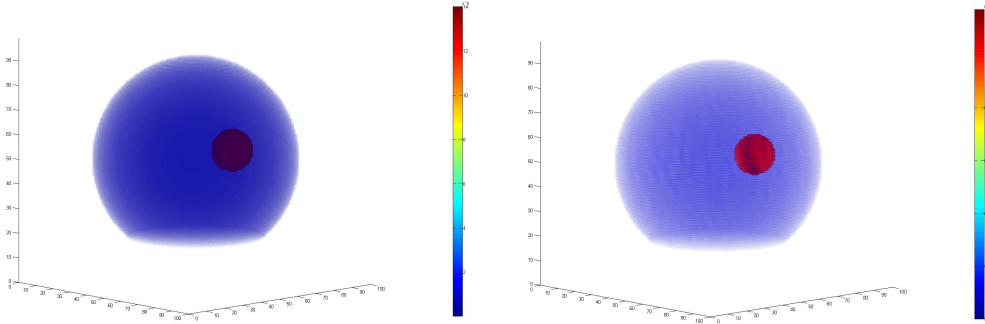


Figure 4: On the left is the original distribution of the real part of the refractive index; on the right is the reconstructed one.

2.4 Two-dimensional Fresnel Imaging: Modelling

In all of the methods mentioned before, the wave falling on a sample is plane. However, it is also possible to focus the wave on the sample using a zone plate. In this case one has to work with an additional plane - the zone plate plane (it is called source plane further in the text). Propagation formula between any two given planes remains the same. However, as we want to focus the wave, the source wavefront now is spherical and has a phase variation of:

$$\Psi(x, y) = e^{-\frac{i\pi(x^2+y^2)}{\lambda z_F}},$$

where x, y are the coordinates in the source plane and z_F is focusing distance of the zone plate. The intensity is modeled as Gaussian.

However, fast Fourier transform does not work well with rapid phase oscillations. [9] So in the source and far-field plane we work not with wavefunctions, but instead with functions P and Q :

$$P = \Psi_{source} e^{\frac{i\pi(x_{source}^2+y_{source}^2)}{\lambda z_S}}, Q = \Psi_{far-field} e^{-\frac{i\pi(x_{far-field}^2+y_{far-field}^2)}{\lambda z_D}},$$

where z_S is the distance between source and sample planes, and z_D is the distance between sample and detector planes. The algorithm for modelling consists of following steps now:

- 1. Propagate the source P function to the sample plane
- 2. Construct the sample transmission function from the known properties and distribution of the materials in the sample
- 3. Multiply the incident wave function in the sample plane by it (assuming the sample is thin)
- 4. Propagate the result to the detector plane
- 5. Calculate the diffracted intensity by squaring the far-field Q function

Diffracted intensity (with central stop and Poissonian noise) is on the Fig. 5.

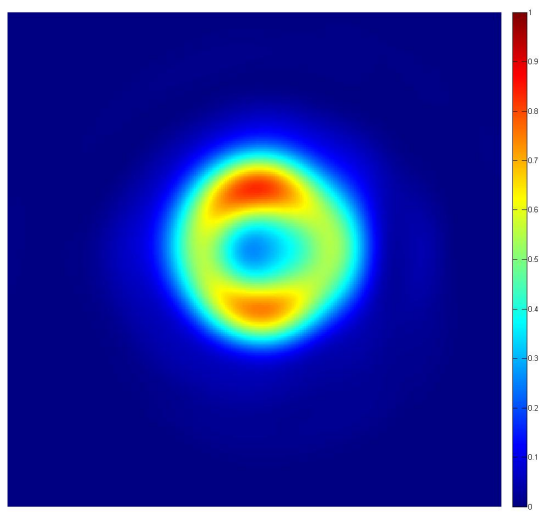


Figure 5: The diffracted intensity with central stop and Poissonian noise applied

3 Conclusions and future work

Modeling of a diffraction pattern for 2D plane wave and Fresnel case is implemented.

HIO&ER iteration algorithm reconstruction in 2D and 3D plane wave case is implemented.

Tomography filtered backprojection reconstruction in plane wave case is implemented.

Further work includes finishing Fresnel case reconstruction and finding optimal working point between noise and radiation damage.

References

- [1] Coherent diffractive imaging of biological samples at synchrotron and free electron laser facilities *A. P. Mancuso & others*
- [2] High-resolution ab initio three-dimensional x-ray diffraction microscopy *Henry N. Chapman & others*
- [3] Neutze, R., et al., 2000. Nature 406, 752
- [4] Emma P., et al., Nature Photonics, 2010
- [5] Howells, M.R., et al., 2009. J. Elect. Spectrosc. Relat. Phenom. 170, 412
- [6] Imaging atomic structure and dynamics with ultrasoft x-ray scattering, K. J. Gaffney, et al. Science 316, 1444 (2007)
- [7] Vartanyantz, I. A., Mancuso, A.P., et al. "Coherence properties of Individual Femtosecond Pulses of an X-Ray Free Electron Laser" arXiv:1105.3898v1 2011
- [8] Bates, R.T.H., 1982. Optik 61, 247
- [9] Fresnel coherent diffractive imaging: treatment and analysis of data. Williams, G.J. et al, New Journal of Physics 12 (2010)
- [10] Advanced Tomographic Methods in Materials Research and Engineering *J. Banhart & others*
- [11] Quiney et al., Nature Physics 2010